Production of “biobetter” variants of glucarpidase with enhanced enzyme activity

Alanod D. Al-Qahtani, Sara S. Bashraheel, Fatma B. Rashidi, C. David O’Connor, Atilio Reyes Romero, Alexander Domling, Sayed K. Goda

Biomedicine & Pharmacotherapy 112 (2019) 108725

Contents lists available at ScienceDirect

Biomedicine & Pharmacotherapy

journal homepage: www.elsevier.com/locate/biopha

Production of "biobetter" variants of glucarpidase with enhanced enzyme activity

Alanod D. Al-Qahtani[a,b,1], Sara S. Bashraheel[a,b,1], Fatma B. Rashidi[c], C. David O'Connor[d], Atilio Reyes Romero[b], Alexander Domling[b], Sayed K. Goda[a,c,*]

[a] Protein Engineering Unit, Life and Science Research Department, Anti-Doping Lab-Qatar (ADLQ), Doha, Qatar
[b] Drug Design Group, Department of Pharmacy, University of Groningen, Groningen, Netherlands
[c] Cairo University, Faculty of Science, Chemistry Department, Giza, Egypt
[d] Department of Biological Sciences, Xi'an Jiaotong-Liverpool University, Science and Education Innovation District, Suzhou 215123, China

ARTICLE INFO

Keywords:
Biobetter glucarpidase
DNA shuffling
Glucarpidase
Error-prone PCR
Drug detoxification
ADEPT
Targeted cancer therapy

ABSTRACT

Glucarpidase, also known as carboxypeptidase G_2, is a Food and Drug Administration-approved enzyme used in targeted cancer strategies such as antibody-directed enzyme prodrug therapy (ADEPT). It is also used in drug detoxification when cancer patients have excessive levels of the anti-cancer agent methotrexate. The application of glucarpidase is limited by its potential immunogenicity and limited catalytic efficiency. To overcome these pitfalls, mutagenesis was applied to the glucarpidase gene of *Pseudomonas* sp. strain RS-16 to isolate three novels "biobetter" variants with higher specific enzyme activity. DNA sequence analysis of the genes for the variants showed that each had a single point mutation, resulting in the amino acid substitutions: I100 T, G123S and T239 A. $K_{m,}$ V_{max} and K_{cat} measurements confirmed that each variant had increased catalytic efficiency relative to wild type glucarpidase.

Additionally, circular dichroism studies indicated that they had a higher alpha-helical content relative to the wild type enzyme. However, three different software packages predicted that they had reduced protein stability, which is consistent with having higher activities as a tradeoff. The novel glucarpidase variants presented in this work could pave the way for more efficient drug detoxification and might allow dose escalation during chemotherapy. They also have the potential to increase the efficiency of ADEPT and to reduce the number of treatment cycles, thereby reducing the risk that patients will develop antibodies to glucarpidase.

1. Introduction

Several strategies for targeted cancer therapy involving glucarpidase, also known as Carboxypeptidase G2 (CPG2), have been put into clinical practice in recent years [1]. (Glucarpidase or CPG2 will be used interchangeably throughout the text).

Glucarpidase has proved particularly useful in Antibody Directed Enzyme Prodrug Therapy (ADEPT), in which it accumulates at the site of a tumor via a tumor-specific antibody, after that it converts a prodrug into an active drug [2–4].

In contrast, in cases of methotrexate-induced toxicity, glucarpidase is administered to convert this anti-cancer agent to a less harmful compound (4-deoxy-4-amino-N10-methylpteroic acid) that is excreted via a hepatic pathway. The enzyme is typically given in high doses to patients, thereby decreasing the risk of renal failure [5–9].

Although clinically useful, patients treated with glucarpidase often develop antibodies against it, which limits the number of times it can be administered.

Additionally, the wild-type enzyme has limited catalytic efficiency and hence must be given in relatively high doses. For both reasons, it would be desirable to develop variants of CPG2 that have increased specific activity but different immunogenic properties due to their altered structures. Such variants might escape recognition by the patients' immune system and might also allow clinicians to decrease the amount of CPG2 that is administered.

The re-assortment of mutations to produce favorable combinations that can undergo natural selection is a critical component of biological evolution. This process can be simulated by directed evolution, which has proved to be an effective strategy for improving or altering the activity of biomolecules for industrial, research and therapeutic

* Corresponding author at: Protein Engineering Unit, Life and Science Research Department, Anti-Doping Lab-Qatar (ADLQ), Doha, Qatar.
E-mail address: sgoda@adlqatar.qa (S.K. Goda).
[1] These two authors contributed equally to the work.

https://doi.org/10.1016/j.biopha.2019.108725
Received 8 January 2019; Received in revised form 13 February 2019; Accepted 21 February 2019

applications. The evolution of proteins in the laboratory uses error-prone DNA replication *in vitro* to generate genetic diversity and specific screens to identify protein variants with desired properties [10]. Where necessary, the genes for these variants can then be shuffled in a process akin to homologous recombination to achieve further improvements [10]. In several instances, chimeric enzymes with improved activity and stability have been isolated from libraries constructed using DNA shuffling [11–14]. In other cases, the method resulted in libraries with either too many mutations in each gene [15] or too few crossovers [16] to be useful.

DNA shuffling can take advantage of orthologous proteins to re-purpose functional diversity from nature, i.e. in addition to using error-prone replication in vitro, it can be used to shuffle distantly related existing sequences to take advantage of the natural diversity that exists within a population and to provide a means to eliminate deleterious mutations that may accumulate in strains [17]. On the other hand, it is limited by the degree of sequence homology shared by the existing sequence variants [10].

This paper describes the production of novel CPG2 variants with increased activity, which may also have structural alterations, and hence altered immunogenicity, thereby allowing additional cycles of therapy. The novel highly active glucarpidase(s) were sub-cloned, overexpressed and functionally characterized.

2. Materials and methods

2.1. Growth media, enzymes, chemicals and antibodies

LB Media was from Formedium (Norfolk, UK) and where necessary was solidified with 1.5% (w/v) Bacto-agar (Fermentas; Waltham, Massachusetts, USA). Enzymes for cloning and expression of the glucarpidase genes were purchased from Thermo Scientific, with the exception of *Sau*3AI, *Bam*H1 and a PCR master mix (2×) kit, which was purchased from Promega (Fitchburg, Wisconsin, USA). Ni-NTA resin was purchased from Sigma-Aldrich (Saint Louis, Missouri, USA). GilPilot 1 kb DNA ladder (100) was purchased from Thermo Scientific (Waltham, Massachusetts, USA), Wizard® SV Gel and PCR Clean-Up System Kit were purchased from Promega. GeneJET Plasmid Miniprep Kit was obtained from Thermo Scientific. All other chemicals were of a high analytical grade. The mass spectroscopy (MS) analysis was carried out at the Toxicology and Multipurpose Labs, ADL-Qatar. Anti-Xen CPG2 Polyclonal Antibodies were produced by Eurogentec, Belgium, anti-Rabbit IgG (whole molecule)–Peroxidase antibody produced in goat (Sigma-Aldrich) was used as secondary conjugated antibody. 6× His Epitope Tag Antibody (HIS. H8) (Thermo Scientific) was used for detection of the purified 6-His-tagged CPG2 and Polyclonal Rabbit Anti-Mouse Immunoglobulins/HRP (Dako Labs, Santa Clara, California, USA) was used as the secondary antibody.

2.2. Mutagenesis and recombination by DNA shuffling

DNA shuffling was carried out essentially according to the Stemmer method [18] using as a template a synthetic version of the CPG2/glucarpidase gene from *Pseudomonas putida* that had been codon-optimized for expression in *E. coli* [19]. First, to enhance the natural mutation rate, libraries of glucarpidase mutants were constructed by error-prone PCR. 30 pmol of each primer flanking the glucarpidase gene set (CPGF; 5′-ACC GGA TCC CAT ATG GCG CTG GCC CAG AAA CG-3′, and CPGR 5-CTT AAG CTT TTA TTT GCC CGC ACC CAG ATC C-3′), 5 mM $MgCl_2$, 0.2 mM of each dATP and dGTP, 1 mM of each dTTP and dCTP, and 0.5 µl *Taq* polymerase was used in the PCR reactions. The thermal cycling parameters were: 95 °C for 2 min (1 cycle), 95 °C for 1 min, 55 °C for 1 min, 72 °C for 2 min (30 cycles) and 72 °C for 5 min (1 cycle). The PCR products were purified using a PCR purification kit (Thermo Scientific). 44 µl of purified DNA template was then mixed with 2.5 µl of 1 M Tris − HCl (pH 7.5), 2.5 µl of 200 mM $MnCl_2$ and brought to a final volume of 49 µl with deionized water. The mixture was equilibrated at 15 °C for 5 min. Subsequently, 1 µl DNase I (10 U/µl) diluted to 1:100 in deionized water for digestion at 15 °C was added. Aliquots (10 µl) was taken after 30 s, 1, 2, 3 and 5 min of incubation and immediately mixed with 5 µl of ice-cold stop buffer containing 50 mM EDTA and 30% (v/v) glycerol. Large scale DNase digest was carried out and the fragments were separated by electrophoresis in 2% agarose gels and DNA fragments in the 200-300bp size range were cut from the gel and extracted. Then, a primerless PCR reaction was carried out, in which 10 µl of purified fragments were combined with 5 µl of 10× *Pfu* buffer, 5 µl of 10× dNTP mixture (2 mM of each dNTP) and 0.5 µl of *Pfu* polymerase to a total volume of 50 µl and then PCR reaction was performed. PCR conditions were: 1 cycle at 95 °C for 3 min, 40 cycles of 95 °C for 30 s, 55 °C for 1 min, 72 °C for 1 min + 5 (s per cycle) and 72 °C for 5 min (1 cycle). Recombinant genes were amplified in a standard PCR reaction using serial dilutions of the assembly reaction. The PCR reaction conditions were: 1 µl serial diluted templates, 10 pmol of each primer set, 5 µl of 10× *Pfu* buffer, 1 µl of 10× dNTP mixture (2 mM of each dNTP) and 0.5 µl of *Pfu* polymerase in the total volume of 50 µl. The thermal cycling parameters was 95 °C for 2 min (1 cycle), 95 °C for 1 min, 55 °C for 1 min, 72 °C for 2 min (30 cycles) and 72 °C for 5 min (1 cycle).

2.3. Sub-cloning of shuffled glucarpidase (S-glucarpidase) mutants

The PCR products were purified using a gel extraction kit (Thermo Scientific) and double-digested with the restriction enzymes *Nde*I and *Hind*III. After further gel purification, the digested glucarpidase gene fragments were ligated into the *Nde*I/*Hind*III sites of the pET28a expression vector and transformed into competent *E. coli*. Plasmid minipreps were purified and sequenced using T7 promoter and terminator primers to screen for mutations.

2.4. Screening for functional S-glucarpidase(s)

Derivatives of the expression vector pET28a expression vector containing variant genes for the shuffled glucarpidase (variants) were selected, transformed into the expression host *E. coli* BL21(DE3) RIL, and then plated on LB/agar plates containing 0.1 mM isopropyl-β-D-thiogalactopyranoside (IPTG), folate and the required antibiotics. The plates were incubated at 37 °C overnight, and colonies that were surrounded by clear zones were selected for protein expression and activity assays using cell-free extracts, as previously described. [20] Priority was given to colonies with large ‘halo zones’, on the assumption that these either produced more glucarpidase or corresponded to variants with increased enzymatic activity.

2.5. Recombinant protein expression and characterization

E. coli BL21(DE3) RIL cells contain pET28a-CPG2, or the same expression vector contain a variant, were incubated with shaking (200 rpm) at 37 °C in 250 ml of LB medium supplemented kanamycin and chloramphenicol (both at 32 µg/ml) until the optical density at 600 nm reached 0.5-0.6. Induction of expression of recombinant CPG2 was initiated by the addition of IPTG at a final concentration of 1 mM, whereupon the culture was incubated for a further four hours at 37 °C with shaking. Cells were collected by centrifugation at 4000 rpm for 20 min at 4 °C and the pellets were re-suspended in Tris buffer (pH 7.5), 50 mM NaCl. Lysis was achieved by sonication, using Soniprep 150 plus, on ice (5 cycles of 30 s sonication pulses followed by 1 min rest). The soluble fraction was separated by centrifugation at 14,000 rpm for 20 min at 4 °C. The soluble and insoluble fractions were mixed with 2× sample buffer, boiled for ten minutes at 95 °C, and then analyzed by SDS-PAGE. Protein expression in cells incubated at 20 °C was carried out identically to assess the effect of temperature on improving soluble protein expression.

2.6. Purification using nickel affinity chromatography

Protein extracts from *E. coli* BL21 (DE3) RIL cells containing pET28a-CPG2, or the same expression vector containing a variant, were subjected to purification by Ni^{2+} affinity chromatography using Ni-NTA resin. About 1 ml of the resin was washed with distilled water and activated by binding and washing buffer A (20 mM Tris pH 8, 50 mM NaCl, 5 mM β-mercaptoethanol (BME), and 20 mM Imidazole) then the total soluble protein was combined with the activated resin and gently agitated for 20 min at 4 °C to allow the protein to bind to the column resin. The resin was separated by gravity, the flow-through was collected, and the resin was washed 3 times with buffer A. The target protein (bound to the resin) was collected by adding ice-cold elution buffer B (20 mM Tris pH 8, 50 mM NaCl, 5 mM BME and 400 mM Imidazole). The eluted protein was dialyzed against 100 mM Tris − HCl pH 7.3 containing 0.2 mM $ZnSO_4$. All fractions from the protein purification were analyzed by SDS-PAGE. MTX hydrolysis the pure recombinant glucarpidase was assayed using as described below.

2.7. Assay of wild-type and mutant glucarpidase activity using methotrexate

The glucarpidase activity of each of the shuffled variants was determined using MTX as substrate. The assay was a modification of the method described by McCullough [21]. 0.1 M Tris − HCl (pH 7.3), 0.2 mM $ZnSO_4$ was used as a dilution buffer for 5 µl of MTX (0.45 mM, final concentration). After equilibration of the reaction mixture at 37°C for 10 min, a total protein extract from the expressed shuffled variant (50 µg/ml) was added and incubated at 37°C. Samples were taken at 10 min intervals, and the decrease in absorbance at 320 nm was measured using a NANODROP 1000 spectrophotometer (Thermo Scientific). The same protocol was used to analyze the activity of the pure recombinant CPG2 using 3 µg/ml protein. The Michaelis-Menten equation was used for determination of the actual values of K_m, K_{cat}, and V_{max} of each protein using GraphPad PRISM 6 software (San Diego, California, USA). One unit of the enzyme represents the amount of enzyme in mg required for hydrolysis of 1 mM of MTX per min at 37 °C. The enzyme activity per ml of protein was calculated using 8300 as the molar extinction coefficient for MTX.

2.8. Circular dichroism of the shuffled CPG2

a Pre-CD Scanning

The wild-type CPG2 and the three variant proteins were purified and dialyzed against Milli-Q water 4 times, 18 h each, then clarified by centrifugation at 14,000 rpm for 30 min at 4 °C. To measure the protein concentration a NanoDrop 2000 spectrophotometer (Thermo Scientific) was used to achieve the required concentration of about 6 µM for the CD measurement. The extinction coefficients were calculated as ε 24,870 M^{-1} cm^{-1} for the four proteins WT, CPG2I100 T, CPG2T329 A and CPG2G123S.

- Circular Dichroism (CD)

CD measurements were obtained using a Chirascan™ Plus CD Spectrometer (Applied Photophysics). Scanning of the proteins (6 µM, final concentration) in the far UV spectral region (260 to 180 nm) was performed in a rectangular demountable SUPRASIL Quartz cuvette (Hellma®) of 0.2 mm light-path length (sample volume ~70 µl). The applied CD parameters were: bandwidth 1 nm and scan time per point of 0.5 s at 20 °C. Four scans were taken per sample, and the readings were averaged and smoothed using the CD analysis software. The produced spectra were subtracted from an averaged CD spectra of the blank baseline (Milli Q water).

- CD- deconvolution method

Protein secondary structures of the pure shuffled CPG2 were calculated by CD data and the deconvolution analysis using the CDNN (version 2.1) software tool. A spectral range of (180–260 nm) was used for the deconvolution calculation. The number of residues and molecular weight were taken as 394 AAs, with 41.9117, 41.8996, 41.8817, 41.9417 kDa for the WT, CPG2I100 T, CPG2T329 A and CPG2G123S, respectively, and the light-path length of the cuvette used was 0.2 cm.

2.9. Prediction of the impact of the single point mutation on glucarpidase

To find a possible correlation with the results of the activity assays, three software packages, mCSM [22], SDM [23], and DUET [24], were used to predict the effects of the mutations on glucarpidase stability and to generate environment-specific substitution tables (ESST) and thermodynamic stability data for glucarpidase mutants.

2.10. Prediction of Hydrogen bond networking of the mutants

The models were generated using Modeller package [25–28] from the crystal structure of carboxypeptidase G2 (PDB: 1CG2). Polar contacts are depicted in red dotted lines and the picture was rendered with Pymol (Version 2.2 Schrödinger, LLC).

2.11. Statistical analysis

Data are presented as mean ± standard error of the mean (S.E.M) of "3″ observations. All graphs were constructed using GraphPad Prism 6 software (San Diego, CA, USA). Statistical analysis was performed using Student *t*-test or two-way ANOVA as appropriate. P values < 0.05 were considered statistically significant.

3. Results

3.1. Mutagenesis of the glucarpidase gene

Error-prone PCR was used to mutate the CPG2 gene of *Pseudomonas putida*, which has previously been codon-optimised for expression in *E. coli* [20]. The mutated genes were fragmented, and then primer-less and conventional PCR was used in an attempt to produce shuffled DNA, and to amplify full-length genes containing mutations (see Materials and Methods for further details) (Supplemental Fig. S1). Following cloning into the expression vector pET28a, DNA sequence analysis was used to confirm mutation and shuffling of the CPG2 gene (data not shown).

3.2. Isolation of variants with enhanced CPG2 activity

pET28a plasmids containing CPG2 variants were transformed into BL21(DE3)RIL and screened for glucarpidase activity on folate-containing agar plates. Approximately four thousand colonies containing variants were screened for hydrolysis of folate by searching for clear zones and yellow precipitates around colonies. 73% of the four thousand colonies grown on folate containing media plates formed clear zones and, of this set, three colonies displayed a significantly darker coloration after two days of incubation relative to cells harboring the original pET28a-CPG2 construct (Supplemental Fig. S2). This suggested that the isolates either produced more glucarpidase or that the glucarpidase in question had a higher level of activity against the folate substrate.

The mutations in the CPG2 genes of three variants that were selected for the further study were identified by sequencing (Supplemental Fig. S3). Each mutant had a single but different codon change relative to the wild-type CPG2 sequence, corresponding to the following amino acid changes: C100 T, G123S, and T329 A. Accordingly, the mutants were named CPG2I100 T, CPG2G123S, and CPG2T329 A.

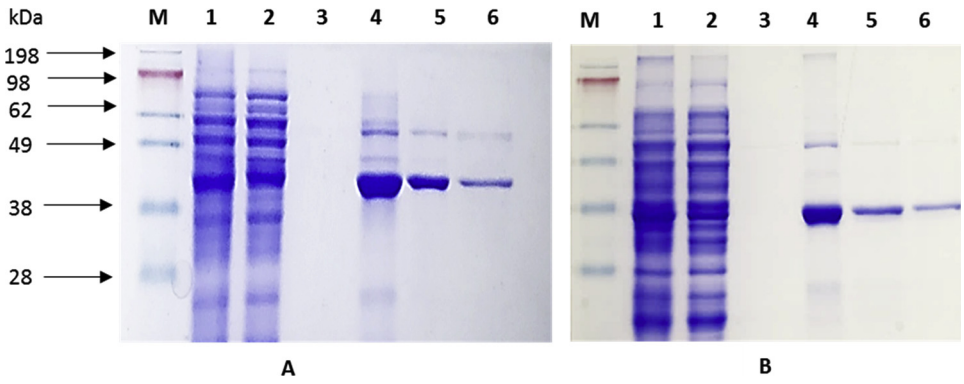

Fig. 1. Ni-NTA Protein purification of CPG2 (*P. putida* and one of the shuffled variant, I100 T) in Bl21(DE3)RIL. A. protein purification of *P. putida* CPG2, and B. an example of a protein purification of a mutant protein, where M is SeeBlue Plus2 Pre-Stained Protein Standard (3–198 kDa), lanes 1, 2, 3, 4, 5, and 6 are total soluble, flow-through, wash, and elutions (E1, E2, and E3 for CPG2 of *P. putida*) respectively.

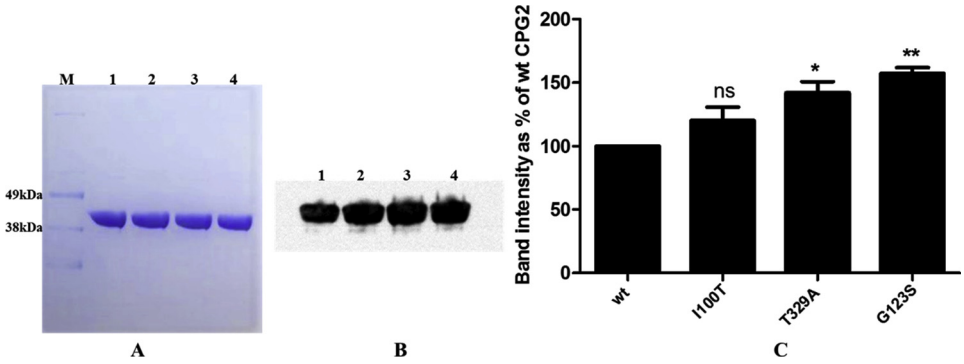

Fig. 2. Western blotting analysis of the shuffled CPG2s relative to WT-CPG2. A) Shows the relevant gel image after SDS-PAGE while B) the corresponding immunoblot. Lanes 1, 2, 3 and 4 are WTCPG2, CPG2I100 T, CPG2T329 A and CPG2G123S, respectively. C) Densitometric quantification of bands was carried using GASepo analysis software. Results are expressed as the percentage of WTCPG2 band intensity and are presented as mean ± standard error of the mean (S.E.M) of 3 independent experiments. Statistically significant difference: *p < 0.05 and **p < 0.01 while ns is not significant. Ex-#1, Ex-#2, and Ex-#3, three independent western blot replicates are shown in the supplement section.

3.3. Purification of the glucarpidase mutants and Western Blot analysis

The three mutant enzymes were overexpressed and purified by affinity chromatography using Ni columns. Fig. 1 shows a representative purification for the wild-type and CPG2 I100 T mutant while Fig. 2 shows the corresponding Western blot analysis using an anti-His antibody.

3.4. Activity of mutant glucarpidases relative to the wild-type enzyme

Equal amounts of protein extracts containing the wild-type and mutant CPG2 enzymes were assayed for glucarpidase activity using MTX as a substrate in the presence of Zn^{2+} ions, as described in the Materials and Methods section. The results indicated that each of the mutants had a higher glucarpidase activity than the wild type enzyme (Fig. 3). The I100 T and G123S mutants showed the largest increases in enzyme activity. However, the T329 A mutant also had a significantly increased activity relative to wild-type CPG2 but less activity than the other two mutants.

Two-way ANOVA statistical analysis of the Enzyme Activity Assay showed a significant difference in activity between the four enzymes $p < 0.001$. When compared with the WTCPG2, there was a significant difference in activity at time 60–780, 150–660 and 180–270 for CPG2I100 T, CPG2G123S and CPG2T329 A, respectively. Details are provided in the (Table 1).

3.5. Kinetic studies of the mutants and comparison with WT-CPG2

More detailed kinetic studies were carried out to characterize the variants further. Specifically, the K_m, V_{max} and K_{cat} values for the

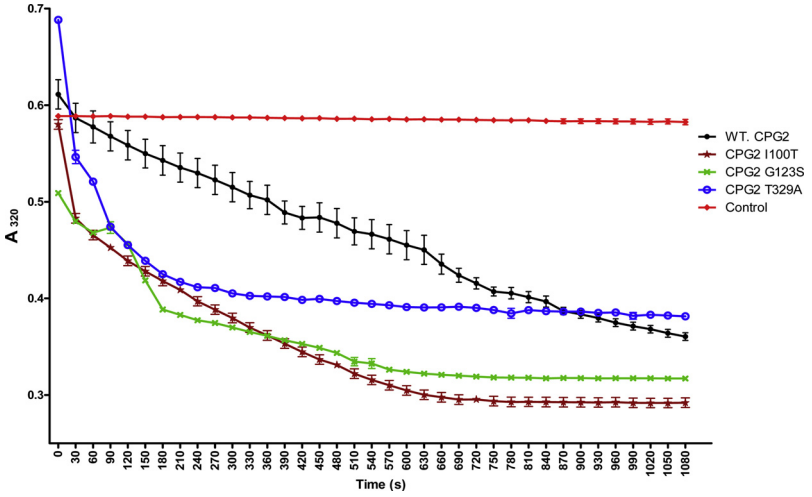

Fig. 3. Activity assay of wild type glucarpidase (wt-CPG2) and the three mutant enzymes using MTX as a substrate. Total protein extracts (50 µg/ml) from cells expressing the proteins were added to MTX (0.45 mM, final concentration), and the change in absorbance at 320 nm recorded. The plot shows the relative activities of WT-CPG2 (black), CPG2I100 T (dark red), CPG2T239 A (blue) and CPG2G123S (Green) in the presence of Zn^{+2} relative to the control in the absence of enzyme (red).

Table 1
The difference in activities between the wild type CPG2 and the three novel mutants and the corresponding p-value.

Time [S]			
WTCPG2 vs CPG2I100T	WTCPG2 vs CPG2G123S	WTCPG2 vs CPG2T329A	P-value
60-210, 720-780	660	180-270	< 0.05
240-510, 660-690	150, 300-630	None	< 0.01
540-630	180-270	None	< 0.001

Table 2
Comparison of the kinetic parameters of the wild-type and mutant CPG2 enzymes using methotrexate as a substrate (± S.E.M, R^2 coefficient of determination).

Enzyme	Kinetic parameter			
	K_m	V_{max}	K_{cat}	R^2
WT CPG2	171.7 ± 65.66	52.6 ± 8.484	24.83 ± 0.9149	0.8791
CPG2 I100T	62.68 ± 10.26	55.34 ± 2.504	26.11 ± 0.3592	0.9317
CPG2 G123S	71.38 ± 13.85	57.69 ± 3.344	27.21 ± 0.4570	0.9123
CPG2 T329A	82.41 ± 15.07	57.09 ± 3.237	26.93 ± 0.4453	0.9175

mutants were determined using methotrexate as a substrate and compared with the wild-type enzyme (Table 2).

3.6. Circular dichroism spectroscopy and secondary structure determination

Given the significant changes in the specific activities of the mutants CPG2 enzymes, it was of interest to see if they also had significant changes in their secondary structures. Accordingly, we obtained and compared CD data in the far UV region for the wild-type and mutant proteins to estimate such changes (Fig. 4). All three of the mutant proteins gave more negative chiral CD signals, relative to the wild-type, in 208–230 nm region. Overall, however, the CPG1I100 T and CPG2G123S mutants had similar profiles to the wild type whereas the CPGT329 A mutant was markedly different. The estimated percentage values for the secondary structure components of the proteins were deduced by CD deconvolution (Table 3). In keeping with the spectral analysis, CPGT329 A was estimated to have significantly more alpha-helical content relative to the other proteins.

The relative amounts of secondary structure in each of the proteins

Table 3
Estimated secondary structure changes in the three mutants relative to the wild-type CPG2 enzyme [1].

	Estimated secondary structure (%)					
	Alpha-helical	Anti-parallel	Parallel	Beta-turn	Random	Total
Wild-type CPG2	34.2	8.5	8.5	16.6	32.3	100
CPG2I100T	36.2	7.6	8.2	16.2	31.5	99.6
CPG2G123S	36.4	7.5	8.1	16.0	31.7	99.7
CPG2T329A	40.7	6.6	7.2	15.5	28.5	98.5

was estimated by CDNN deconvolution analysis using the data shown in Fig. 4. The average values (as percentages) of each secondary structure component for four sets of measurements is shown.

3.7. The impact of the single point mutations on glucarpidase stability

Given the differences in secondary structure indicated by the CD studies, we checked the predicted impact of the amino acid alterations on the stability of the glucarpidase variants (Table 4**)**. Three software packages were used to predict whether the amino acid changes were likely to stabilize or destabilize the protein structure of CPG2. Although programs mostly predicted the changes to be destabilizing, the Site Directed Mutator (SDM) package predicted that T329 A change would be stabilizing.

3.8. Prediction of the hydrogen bond network of glucarpidase mutants

Visual inspection of the predicted models disclosed new hydrogen bond network forming between the mutated amino acids and adjacent residues as shown in the figure panel of Fig. 5.

4. Discussion

Glucarpidase, the recombinant form of CPG2, has been used for more than two decades as a detoxifying agent for MTX and also in targeted cancer therapies such as ADEPT. However, its usefulness in both treatment regimens has been limited by its relatively low specific activity and the fact that patients often develop antibodies against it after repeated administration. In our previous study [29], we successfully produced two long-acting variants of glucarpidase, PEGylated glucarpidase and HSA-fused Glucarpidase. We demonstrated that both

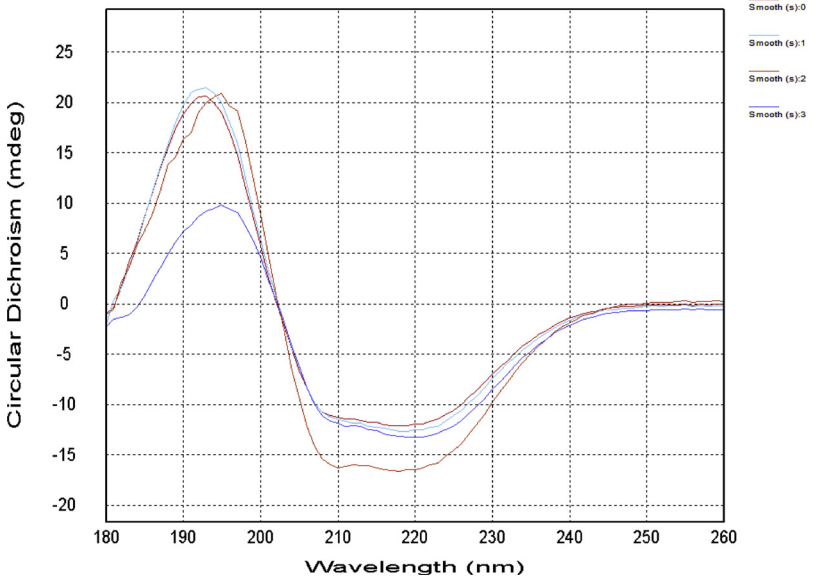

Fig. 4. CD analysis in the far UV region of wt CPG2 and the three mutants. The red, cyan, orange and dark blue curves correspond to wild-type CPG2, CPG1I100 T, CPGT329 A, and CPG2G123S enzymes, respectively. The baseline corrected CD (mdeg) molar ellipticity [Θ] displayed more negative chiral CD signals with shuffled proteins relative to the wild-type enzyme at the same protein concentration (0.58 mg/ml).

Table 4
Predicted stabilities of the mutant CPG2 enzymes.

Program used for predicting stability change	CPG2 I100T ΔΔG	CPG2 G123S ΔΔG	CPG2 T329 A ΔΔG
mCSM [22]	−2.127Kcal/mol (destabilizing)	−2.205 Kcal/mol (destabilizing)	−0.535 Kcal/mol (destabilizing)
SDM [23]	−2.66 Kcal/mol (destabilizing)	−2.23 Kcal/mol (destabilizing)	0.16 Kcal/mol (stabilizing)
DUET [24]	−2.34 Kcal/mol (destabilizing)	−2.246Kcal/mol (destabilizing)	−0.283 Kcal/mol (destabilizing)

"biobetter" glucarpidases are less immunogenic and had prolonged half-lives relative to the native enzyme. However, the study did not address the question of the native enzymes relatively low specific activity. In the present work, we used mutagenesis techniques to produce further "biobetter" glucarpidase variants with improved activity.

Following mutagenesis of the glucarpidase gene of *Pseudomonas* sp. strain RS-16 [30], approximately 73% of the clones retained enzyme activity, as indicated by the clear zones and yellow precipitate surrounding their colonies. However, there were very few that had 'halos' around colonies that were darker than that of the wild-type, which would be indicative either of more active glucarpidase variants or variants that over-produced the enzyme relative to the wild-type construct. DNA sequence analysis of the three mutants taken for further study indicated that each had a single point mutation leading to the alteration of a single amino acid at the protein level (Supplemental Fig. S3). The fact that only single point mutations were present suggests that the error-prone PCR may have contributed more than the DNA shuffling procedure to the production of these particular mutants. Alternatively, it is possible that combining two or more individual mutations into a single gene may have resulted in mutant enzymes with little or no enzyme activity.

The three mutant enzymes, named CPG2 I100 T, CPG2 G123S, and CPG2 T329 A, were then characterized in greater detail. In keeping with their colony phenotypes, each had a higher specific activity in enzyme assays, and this was supported by the results of studies to determine their kinetic parameters. Specifically, the three mutants had higher substrate affinity as shown by their lower K_m values relative to the wild-type enzyme (Table 2). It remains to be seen if combining two or more of the mutations into the same CPG2 gene results in a further increase in enzyme activity.

Having established that the mutants had increased enzyme activity against the substrate MTX, it was then of interest to determine the extent to which their structures had been perturbed. Accordingly, we carried out a CD study to check for alterations in secondary structure, and also analyzed their predicted amino acid sequences using programs designed to predict changes in protein stability. For two of the mutants, CPG2 I100 T and CPG2 G123S, the alterations in secondary structure appear to be modest although it is likely that they are slightly destabilizing.

The analysis of the three web servers to predict the effect of a single mutant [22–24], the prediction shows a higher destabilizing effect in position 100 and 123 compared to 329 of the three mutants. In contrast, CD analysis of the third mutant, CPG2 T329 A, suggests that it has a marked increase in alpha-helical content, which, interestingly, might even lead to a modest increase in its structural stability, as indicated by analysis with the SDM software package (Table 4).

It has previously been shown [31] that amino acids in a protein that is involved in enzyme catalysis are not optimized for stability. Thus, replacement of specific residues may reduce the activity of an enzyme but concomitantly increase its stability. Alternatively, the replacement of residues involved in protein stability could lead to higher enzyme activity. The results presented in this work are consistent with these findings. The three randomly produced glucarpidase mutation substitution, I100 T, G123S and T329 A, increased the enzyme activity in each case but are predicted to decrease the stability of each mutant (Fig. 3, Table 4).

Our study may also suggest the involvement of the isoleucine, glycine and alanine at positions 100, 123 and 329, respectively, in glucarpidase catalysis. It has previously been shown that [32] proteins with specific sites known as flexibility hotspots are important for both binding and stability.

The predicted structure (Fig. 5) shows that in the two mutations, I100 T and G123S, hydrophobic and neutral side chains respectively, are replaced replace with a polar functional group. As previously

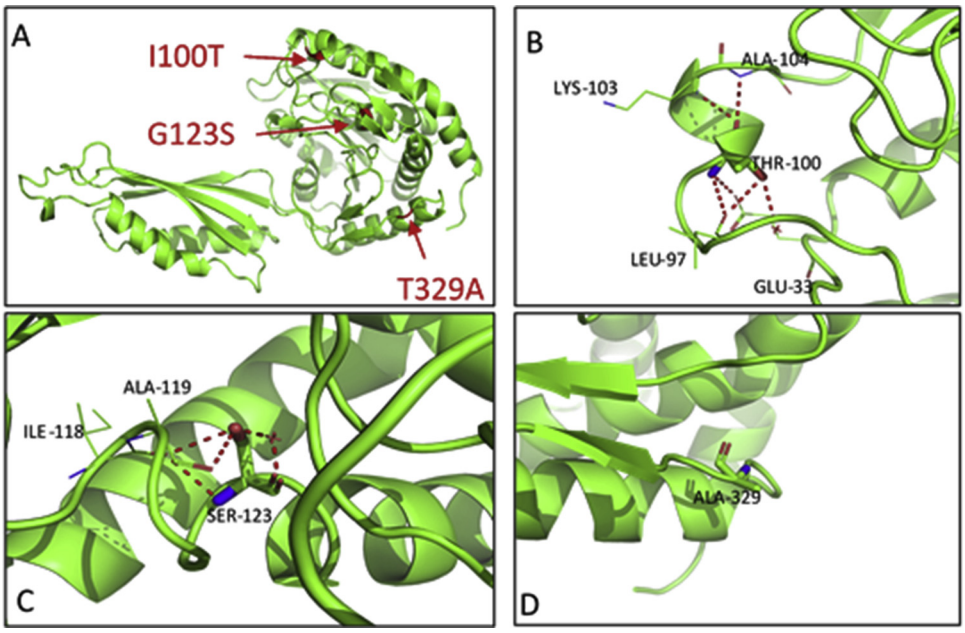

Fig. 5. Figure panel is showing the modelled prediction of hydrogen bond network following point mutation in the various mutants. (A) Cartoon representation of chain A of glucarpidase. Red arrows indicate where the single point mutations were made. (B) Compared to the native type, the mutant I100 T acquires a new hydrogen bond between the hydroxyl group of threonine and the carboxyl group of Leu-97. (C) The mutant G123S forms a hydrogen bond with Ile-118 similarly to the unmutated form but interacts with Ala-119 and loses the hydrogen bond with Val-127. (D) On the contrary, in mutant T329 A no extra hydrogen bonds with neighbored residues were observed.

observed [33], only certain amino acids show a specific propensity to become part of an alpha helix [33]: according to the proposed scale, the helical penalty of threonine and serine are 0.66 Kcal/mol and 0.50 Kcal/mol. Such thermodynamic penalties can be related to steric clashes and the formation of new hydrogen bonds, as we propose in our models. The substitution with such amino acids can therefore lead to a destabilization to the wild type, and this reinforces the validity of the model calculated for the I100 T and G123S which were found to be more active to cleave the methotrexate compared to T329 A.

Further information on these points will probably require X-Ray crystallographic or NMR studies on the mutants. Such studies might also open a rational pathway for further changes to produce other variants with different features.

5. Conclusion

In this study, we produced three novel glucarpidase variants with improved enzyme activity. The mutants may be beneficial in MTX detoxification and may also have applications in targeted cancer strategies such as ADEPT.

Conflict of interest

All authors declare that they have no conflict of interest

Author contribution

ADA and SSB designed the experiment under the supervision of AD and SG, performed the experiments and analyzed the data and wrote the first draft: FBR, performed experimental work, supervision, and contributed to the data analysis. ARR performed the X ray prediction work, DOC, writing – review & editing the manuscript, AD and SKG supervised the work, and SKG the overall supervision of the project

All authors discussed the manuscript and approved it for publications.

Acknowledgements

QNRF grant number NPRP6-065-3-012, Qatar National Research Fund, Doha Qatar for funding this work with grant number NPRP No.: NPRP6-065-3-012.

Appendix A. Supplementary data

Supplementary material related to this article can be found, in the online version, at doi:https://doi.org/10.1016/j.biopha.2019.108725.

References

[1] P.J. Burke, The potential use of carboxypeptidase G2 in the treatment of cancer, Expert Opin. Ther. Pat. 10 (2) (2000) 209–214, https://doi.org/10.1517/13543776.10.2.209.

[2] S.K. Sharma, K.D. Bagshawe, Antibody directed enzyme prodrug therapy (ADEPT): trials and tribulations, Adv. Drug Deliv. Rev. 118 (2017) 2–7, https://doi.org/10.1016/j.addr.2017.09.009 PubMed PMID: 28916498.

[3] S.K. Sharma, K.D. Bagshawe, Translating antibody directed enzyme prodrug therapy (ADEPT) and prospects for combination, Expert Opin. Biol. Ther. 17 (1) (2017) 1–13, https://doi.org/10.1080/14712598.2017.1247802 PubMed PMID: 27737561.

[4] A.P. Mishra, S. Chandra, R. Tiwari, A. Srivastava, G. Tiwari, Therapeutic potential of prodrugs towards targeted drug delivery, Open Med. Chem. J. 12 (2018) 111–123, https://doi.org/10.2174/1874104501812010111 PubMed PMID: 30505359; PubMed Central PMCID: PMCPMC6210501.

[5] M. Mohty, H. Peyriere, C. Guinet, D. Hillaire-Buys, J.P. Blayac, J.F. Rossi, Carboxypeptidase G2 rescue in delayed methotrexate elimination in renal failure, Leuk. Lymphoma 37 (3-4) (2000) 441–443, https://doi.org/10.3109/10428190009089446 PubMed PMID: 10752997. Epub 2000/04/07.

[6] S. Buchen, D. Ngampolo, R.G. Melton, C. Hasan, A. Zoubek, G. Henze, et al., Carboxypeptidase G2 rescue in patients with methotrexate intoxication and renal failure, Br. J. Cancer 92 (2005) 480, https://doi.org/10.1038/sj.bjc.6602337.

[7] L.B.B.F. Ramsey, M.M. O'Brien, K. Schmiegelow, J.L. Pauley, A. Bleyer, B.C. Widemann, D. Askenazi, S. Bergeron, A. Shirali, S. Schwartz, A.A. Vinks, J. Heldrup, Consensus guideline for use of glucarpidase in patients with high-dose methotrexate induced acute kidney injury and delayed methotrexate clearance, Oncologist 23 (Jan (1)) (2018) 52–61, https://doi.org/10.1634/theoncologist.2017-0243.

[8] Dijkman M.A. dLD, I. de Vries, Do not exclude glucarpidase too soon in the context of high-dose methotrexate induced nephrotoxicity, Neth. J. Med. 76 (May (4)) (2018) 204.

[9] H.L.V. Garcia, F. Goldwasser, D. Bouscary, E. Raffoux, N. Boissel, S. Broutin, D. Joly, Renal toxicity of high-dose methotrexate, Nephrol. Ther. 14 (April (Suppl 1)) (2018) S103, https://doi.org/10.1016/j.nephro.2018.02.015.

[10] M.S. Packer, D.R. Liu, Methods for the directed evolution of proteins, Nat. Rev. Genet. 16 (2015) 379, https://doi.org/10.1038/nrg3927.

[11] C.C. Chang, T.T. Chen, B.W. Cox, G.N. Dawes, W.P. Stemmer, J. Punnonen, et al., Evolution of a cytokine using DNA family shuffling, Nat. Biotechnol. 17 (8) (1999) 793–797, https://doi.org/10.1038/11737 Epub 1999/08/03PubMed PMID: 10429246.

[12] J.E. Ness, M. Welch, L. Giver, M. Bueno, J.R. Cherry, T.V. Borchert, et al., DNA shuffling of subgenomic sequences of subtilisin, Nat. Biotechnol. 17 (9) (1999) 893–896, https://doi.org/10.1038/12884 Epub 1999/09/03PubMed PMID: 10471932.

[13] F.C. Christians, L. Scapozza, A. Crameri, G. Folkers, W.P. Stemmer, Directed evolution of thymidine kinase for AZT phosphorylation using DNA family shuffling, Nat. Biotechnol. 17 (3) (1999) 259–264 Epub 1999/03/30. doi: 10.1038/7003. PubMed PMID: 10096293.

[14] F. Bruhlmann, W. Chen, Tuning biphenyl dioxygenase for extended substrate specificity, Biotechnol. Bioeng. 63 (5) (1999) 544–551 Epub 1999/07/09. PubMed PMID: 10397810.

[15] H. Zhao, F.H. Arnold, Optimization of DNA shuffling for high fidelity recombination, Nucleic Acids Res. 25 (6) (1997) 1307–1308 Epub 1997/03/15. PubMed PMID: 9092645; PubMed Central PMCID: PMCPMC146579.

[16] M. Kikuchi, K. Ohnishi, S. Harayama, Novel family shuffling methods for the in vitro evolution of enzymes, Gene 236 (1) (1999) 159–167 Epub 1999/08/06. PubMed PMID: 10433977.

[17] Q.-Q. Tong, Y.-H. Zhou, X.-S. Chen, J.-Y. Wu, P. Wei, L.-X. Yuan, et al., Genome shuffling and ribosome engineering of Streptomyces virginiae for improved virginiamycin production, Bioprocess Biosyst. Eng. 41 (5) (2018) 729–738, https://doi.org/10.1007/s00449-018-1906-3.

[18] W.P. Stemmer, DNA shuffling by random fragmentation and reassembly: in vitro recombination for molecular evolution, Proc. Natl. Acad. Sci. U. S. A. 91 (22) (1994) 10747–10751 Epub 1994/10/25. PubMed PMID: 7938023; PubMed Central PMCID: PMCPMC45099.

[19] S.K. Goda, F.A. Rashidi, A.A. Fakharo, A. Al-Obaidli, Functional overexpression and purification of a codon optimized synthetic glucarpidase (carboxypeptidase G2) in Escherichia coli, Protein J. 28 (9-10) (2009) 435, https://doi.org/10.1007/s10930-009-9211-2 Epub 2009/11/17. PubMed PMID: 19911261.

[20] F.B. Rashidi, A.D. AlQhatani, S.S. Bashraheel, S. Shaabani, M.R. Groves, A. Dömling, et al., Isolation and molecular characterization of novel glucarpidases: enzymes to improve the antibody directed enzyme pro-drug therapy for cancer treatment, PLoS One 13 (4) (2018) e0196254, , https://doi.org/10.1371/journal.pone.0196254 PubMed PMID: PMC5919439..

[21] J.L. McCullough, B.A. Chabner, J.R. Bertino, Purification and properties of carboxypeptidase G 1, J. Biol. Chem. 246 (23) (1971) 7207–7213 Epub 1971/12/10. PubMed PMID: 5129727.

[22] Blundell T.L. Pires DE AD, mCSM: predicting the effects of mutations in proteins using graph-based signatures, Bioinformatics 30 (3) (2014) 335–342, https://doi.org/10.1093/bioinformatics/btt691.

[23] A.P. Pandurangan, B. Ochoa-Montano, D.B. Ascher, T.L. Blundell, SDM: a server for predicting effects of mutations on protein stability, Nucleic Acids Res. 45 (W1) (2017) W229–w35, https://doi.org/10.1093/nar/gkx439 Epub 2017/05/20 PubMed PMID: 28525590; PubMed Central PMCID: PMCPMC5793720.

[24] D.E.A.D. Pires, T.L. Blundell, DUET: a server for predicting effects of mutations on protein stability using an integrated computational approach, Nucleic Acids Res. 42 (web Server issue) (2014) W314–W319, https://doi.org/10.1093/nar/gku411.

[25] A. Sali, T.L. Blundell, Comparative protein modelling by satisfaction of spatial restraints, J. Mol. Biol. 234 (3) (1993) 779–815, https://doi.org/10.1006/jmbi.1993.1626 Epub 1993/12/05PubMed PMID: 8254673.

[26] M.A. Marti-Renom, A.C. Stuart, A. Fiser, R. Sanchez, F. Melo, A. Sali, Comparative protein structure modeling of genes and genomes, Annu. Rev. Biophys. Biomol. Struct. 29 (2000) 291–325, https://doi.org/10.1146/annurev.biophys.29.1.291 Epub 2000/08/15.PubMed PMID: 10940251.

[27] A. Fiser, R.K. Do, A. Sali, Modeling of loops in protein structures, Protein Sci. 9 (9) (2000) 1753–1773, https://doi.org/10.1110/ps.9.9.1753 Epub 2000/10/25 PubMed PMID: 11045621; PubMed Central PMCID: PMCPMC2144714..

[28] B. Webb, A. Sali, Protein structure modeling with MODELLER, Methods Mol. Biol. 1654 (2017) 39–54, https://doi.org/10.1007/978-1-4939-7231-9_4 Epub 2017/10/08. PubMed PMID: 28986782.

[29] A.D. AlQahtani, L. Al-Mansoori, S.S. Bashraheel, F.B. Rashidi, A. Al-Yafei, P. Elsinga, et al., Production of "biobetter" glucarpidase variants to improve drug detoxification and antibody directed enzyme prodrug therapy for cancer treatment, Eur. J. Pharm. Sci. 127 (2018) 79–91, https://doi.org/10.1016/j.ejps.2018.10.014 Epub 2018/10/22.PubMed PMID: 30343151.

[30] N.P. Minton, T. Atkinson, R.F. Sherwood, Molecular cloning of the Pseudomonas carboxypeptidase G2 gene and its expression in Escherichia coli and Pseudomonas putida, J. Bacteriol. 156 (3) (1983) 1222–1227 Epub 1983/12/01. PubMed PMID: 6358192; PubMed Central PMCID: PMCPMC217971.

[31] N.S.F. Tokuriki, L. Serrano, D.S. Tawfik, How protein stability and new functions trade off, PLoS Comput. Biol. 4 (2) (2008) e1000002, , https://doi.org/10.1371/journal.pcbi.1000002.
[32] K. Teilum, J.G. Olsen, B.B. Kragelund, Protein stability, flexibility and function, Biochim. Biophys. Acta 1814 (8) (2011) 969–976, https://doi.org/10.1016/j.bbapap.2010.11.005 Epub 2010/11/26. PubMed PMID: 21094283.
[33] C.N. Pace, J.M. Scholtz, A helix propensity scale based on experimental studies of peptides and proteins, Biophys. J. 75 (1) (1998) 422–427 Epub 1998/07/02. PubMed PMID: 9649402; PubMed Central PMCID: PMCPMC1299714.